Fragility Evaluation with Aleatory and Epistemic Uncertainty against Fault Displacement for Reactor Buildings

Hirokazu Tsuji[a], Minoru Kanechika[b], Yoshinori Mihara[b], and Kenshiro Ishiki[b]*
[a] Japan Nuclear Safety Institute, Tokyo, Japan
[b] Kajima Corporation, Tokyo, Japan
*ishikik@kajima.com

Abstract: The Japan Nuclear Safety Institute had recently reported the pioneering deterministic evaluation approach for nuclear power plants under seismic-induced fault displacement. But the uncertainty of fault displacement based on probabilistic hazard analysis is described to be greater than that of other natural phenomena, for example, earthquake ground motions or seismic acceleration vibration in the report. Furthermore, for plant-wide risk assessment against fault displacement hazards beyond the design basis displacement level, it is seriously necessary to promote a series of fundamental studies and develop standard procedures regarding not only accident sequence analysis but also fragility analysis of buildings and structures, as well as components and piping systems. Based on the above background, the objective of this study is to obtain basic fragility data for the aleatory and epistemic uncertainties of structural responses for nuclear power plant buildings against fault displacement. A number of nonlinear soil-structure finite element analyses against relatively large fault displacement have been performed with the randomness of soil and building material properties, the uncertainty of contact parameters relating to friction between soil and building, and the uncertainty of fault hazards such as fault types and geometries. Their quantitative results for fragility data are shown in this paper.

Keywords: Fault Displacement Hazard, Secondary Fault, Reactor Building, Fragility Evaluation

1. INTRODUCTION

New Japanese safety regulations enforced in 2013 require that nuclear power plant facilities with important safety functions shall be established on ground that has been confirmed to have no outcrop of a capable fault, etc., to prevent the risk of fault displacement or other soil movements damaging buildings and equipment therein, and on-site fault assessment is a big issue in the regulatory process. Thus, the Japan Nuclear Safety Institute (JANSI) established an On-site Fault Assessment Method Review Committee, which has proposed a procedure for comprehensive assessment of plant safety against fault displacement based on scientific and engineering knowledge. JANSI has been domestically and internationally reporting a pioneering deterministic approach to evaluating the safety of nuclear power plants against fault displacement [1].

The JANSI report does not focus only on whether an on-site fault may be an active fault. Rather, it is intended to show the scientific and engineering framework to examine whether it has a significant impact on the safety functions of important nuclear power plant facilities when there is ground deformation due to fault movement in the ground on which they are sited. The report also demonstrates preliminary reactor building responses against an assumed fault displacement of 30 cm, which is based on the largest values of secondary faults from approximately 120 years of data in Japan with reference to a survey in the report. But the report describes the uncertainty of fault displacement based on probabilistic hazard analysis to be greater than that of other natural phenomena, such as earthquake ground motions and seismic acceleration vibrations. Furthermore, for plant-wide risk assessment against fault displacement hazards beyond the largest recorded value, it is necessary to promote a series of fundamental studies and to develop standard procedures for not only accident sequence analysis but also fragility analysis of buildings and structures, as well as components and piping systems.

Thus, the objective of this paper is to obtain basic fragility data for aleatory and epistemic uncertainties of structural responses for nuclear power plant buildings against fault displacement. A number of nonlinear soil-structure finite element analyses against relatively large fault displacements are performed considering the randomness of soil and building material properties, the uncertainty of contact parameters relating to friction between soil and building, and also the uncertainty of fault hazards such as fault types and geometries. Now, the study of aleatory uncertainties is based on a probabilistic method, for example, the two-point estimation method, but the study of epistemic uncertainties is deterministic. This paper first presents quantitative results for fragility data. Then, for plant-wide risk assessment from the defense-in-depth viewpoint, it also presents a preliminary fragility evaluation of base mat slabs against fault displacement beyond the largest recorded value of 30 cm. Finally, it describes some technical issues in developing a building fragility evaluation procedure in the future in reference to the tentative failure probability of a reactor building against fault displacement. In addition to the contents already reported [2], the following items are shown in this paper.

- Study of aleatory uncertainties with shear wave velocity of the surface soil and coefficient of friction between soil and building as variables
- Analytical results for hard rock sites
- Fragility evaluation of base mat slabs with the viewpoint of prevention of large-scale damage to containment vessels

2. ANALYTICAL CONDITIONS

The analytical cases are listed in Table 1. For the study on variations of building responses against fault displacement, analytical conditions for the basic case are basically the same as those in the preliminary analysis of a BWR-type reactor building with a soil shear wave velocity Vs = 500 m/s and 1500 m/s in the JANSI report. Details of other cases are explained in later chapters.

The soil-structure interaction finite element model used for analyses is shown in Figure 1. The building model is 80 m square, the base mat slab is 5.5 m thick, and the lower two stories are embedded in soil. The building is modeled by laminated shell elements with 11 integration points in thickness and by beam elements. The soil model is 250 m square and 150 m deep. The fault plane in the basic case is assumed to be a reverse fault with a 60-degree dip angle. The soil is modeled by solid elements.

The material properties of concrete, rebar, and soil are the same as those in the JANSI report. Concrete is assumed at the actual strength, and the nonlinear property of concrete is based on the isotropic

Table 1: Analytical Cases

Case #	Shear wave velocity (support soil)	Shear wave velocity (surface soil)	Strength of concrete	Coefficient of friction	Fault type	Fault position※	Dip angle	Remarks
	m/s	m/s	MPa	-	-	-	°	
0	500	500	44.1	0	Reverse	D/2	60	Basic case
1	459(−σ)	459(−σ)	39.7(−σ)	0	Reverse	D/2	60	Study of Aleatory Uncertainties
2	459(−σ)	459(−σ)	51.4(+σ)	0	Reverse	D/2	60	
3	562(+σ)	562(+σ)	51.4(+σ)	0	Reverse	D/2	60	
4	562(+σ)	562(+σ)	39.7(−σ)	0	Reverse	D/2	60	
5	500	250	44.1	0	Reverse	D/2	60	
6	500	150	44.1	0	Reverse	D/2	60	
7	500	500	44.1	0.8	Reverse	D/2	60	
8	500	500	44.1	1.6	Reverse	D/2	60	
9	500	500	44.1	0	Normal	D/2	60	Study of Epistemic Uncertainties
10	500	500	44.1	0	Reverse	D/4	60	
11	500	500	44.1	0	Reverse	D/2	30	
12	1500	1500	44.1	0	Reverse	D/2	60	Hard Rock Site
13	1500	150	44.1	0	Reverse	D/2	60	
14	1500	1500	44.1	0	Normal	D/2	60	

※The positon of dip-slip fault immediately below base mat slab.（D：width of base mat slab）

Note：The red characters are the main variation parameters.

plastic damage model [3]. The nonlinear property of the rebars is based on isotropic hardening with the von Mises yield surface. The nonlinear property of the soil is based on the Mohr-Coulomb model.

Soil-structure interaction finite element analyses against fault displacement are performed through the two analytical steps shown in Figure 2. In the dead load step, linear elastic analysis is performed for soil and building dead loads. The soil side is assumed to be horizontally fixed and vertically free. The soil bottom is assumed to be vertically fixed and horizontally free. Contact interaction between each fault plane is also assumed to be firmly fixed. In the fault displacement step, after the stresses at the fault plane in the dead load step are completely released, nonlinear elastoplastic analysis is performed for fault displacement. The coefficient of friction is assumed to be zero along the fault plane.

Contact interaction between soil and building is considered only simple contact without friction, except in cases 7 and 8 because of the waterproof layer.

Abaqus Standard Ver. 6 is used for the above soil-structure finite element analyses for fault displacement.

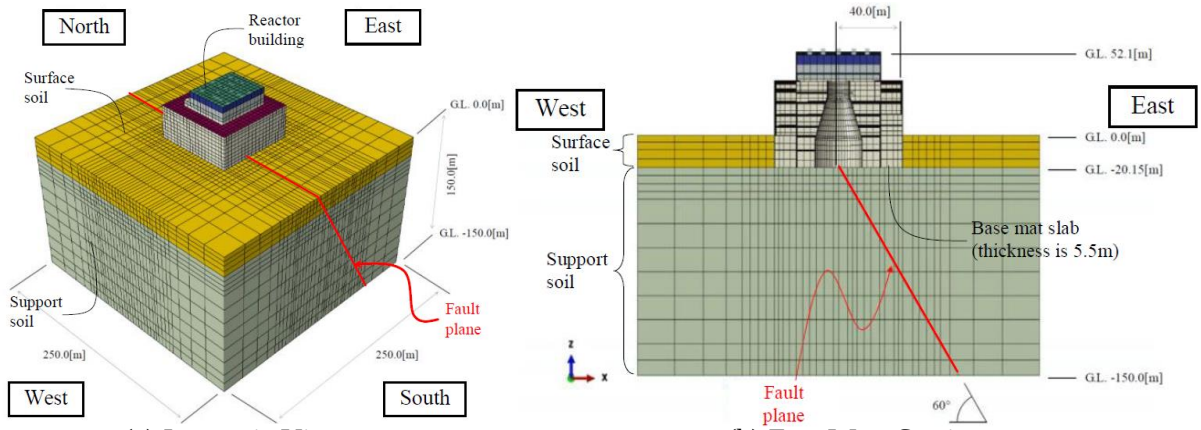

(a) Isometric View (b) East-West Section

Figure 1: Soil-Structure Interaction Finite Element Model

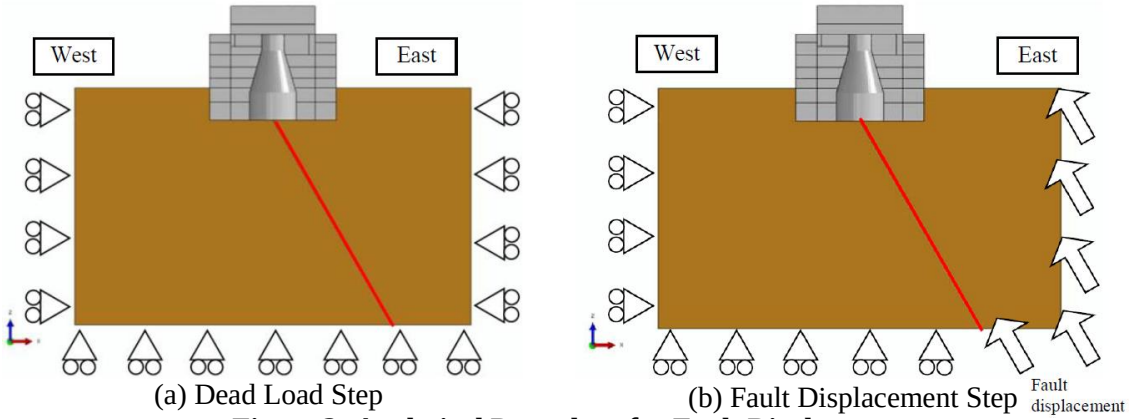

(a) Dead Load Step (b) Fault Displacement Step

Figure 2: Analytical Procedure for Fault Displacement

3. ANALYTICAL RESULTS FOR BASIC CASE

The analytical results are shown in Table 2. For plant-wide risk assessment from the defense-in-depth viewpoint, this paper shows the analytical results for case 0 up to a fault displacement of 60 cm, which is twice the largest recorded value of 30 cm.

The out-of-plane shear stress contour plot in the base mat slab at fault displacement of 60 cm is shown in Figure 3. For out-of-plane shear stress in the base mat slab, it becomes significant beyond fault displacements of 0 cm to 40 cm where the uplift of base mat slab seems to be dominant. Since the

maximum value is about 2.38 MPa immediately above the fault plane, it is lower than the out-of-plane shear capacity of 2.79 MPa based in the previous experimental study [4] even at fault displacement of 60 cm.

Also, all rebars of the base mat slab and the building outer walls are within the elastic limit. On the other hand, for out-of-plane shear stress of building outer walls, the maximum value is about 4.94 MPa where they touch the front and back soil.

Table 2: Analytical Results at Fault Displacement 60 cm

Case #	Base mat slab				Outer walls	Uplift deformation angle
	Concrete		Rebar		Concrete	
	Out-of-plane shear stress	Compressive strain	Tensile strain	Compressive strain	Out-of-plane shear stress	
	MPa	μ	μ	μ	MPa	-
0	2.380	964.1	489.7	804.2	4.941	1/151
5	2.365	874.4	637.5	705.0	2.586	1/129
6	2.434	853.7	818.9	665.7	1.399	1/126
7	1.766	791.1	280.2	680.0	4.063	1/278
8	2.641	884.8	300.4	799.6	4.572	1/269
9	2.843	851.0	1825	548.6	0.5463	1/97
10	2.524	584.2	167.0	520.1	4.781	1/147
11	2.023	778.3	308.4	665.2	3.764	1/211
12	4.210	107100	966.3	94650	23.81	1/612
13	3.381	780.3	518.4	635.4	2.165	1/85
14	5.588	992.6	3132	551.4	1.678	1/79

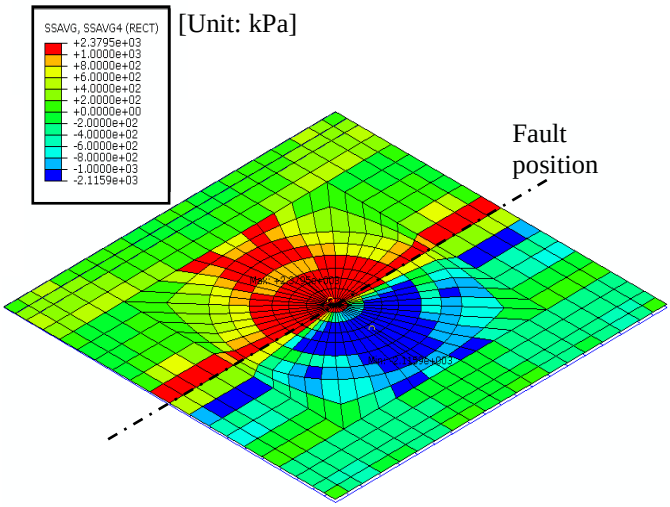

Figure 3: Out-of-plane Shear Stress Normal to Fault

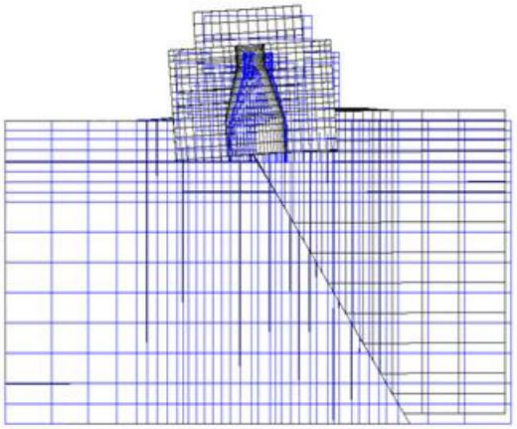

Figure 4: Building Deformation Plot

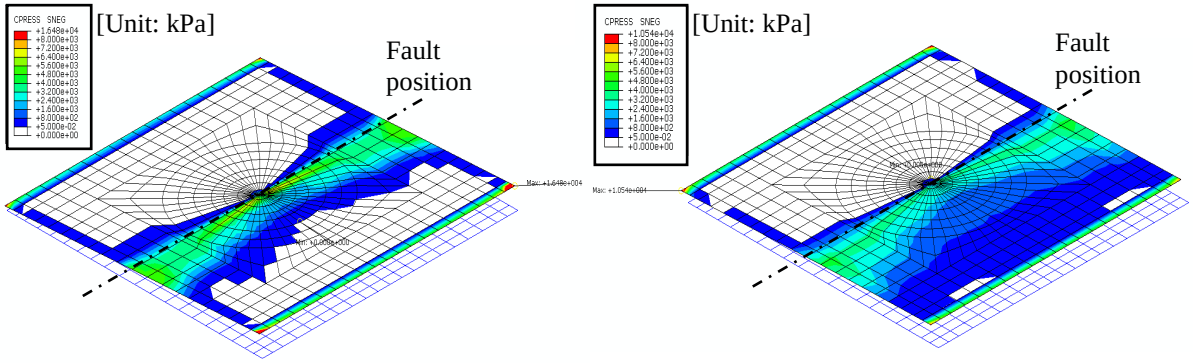

(a) Case 0 (Coefficient of Friction 0.0) (b) Case 7 (Coefficient of Friction 0.8)

Figure 5: Contact Pressure

A building deformation plot at fault displacement of 60 cm is shown in Figure 4, and the contact pressure contour plot of the base mat slab at fault displacement of 60 cm is shown in Figure 5(a). For building deformation, there is no significant uplift of the base mat slab at fault displacement 10 cm. But about half of it is uplifted at fault displacements of 20–30 cm; finally, the building is supported only near the fault plane at fault displacement of 60 cm. The building rotates almost rigidly and its deformation angle is 1/151.

4. STUDY OF ALEATORY UNCERTAINTIES

According to the seismic PRA standard in Japan [5], independent variables to evaluate the variability of building responses against fault displacement are concrete compressive strength and soil shear wave velocity. Their medians and coefficients of variance are also given. The two-point estimation method shown in Table 1 for cases 1 to 4 is applied as a sampling method to calculate the variability of building responses. Other dependent parameters are assumed to be perfectly correlated with the above independent variables.

Based on the two-point estimation method, taking into account the randomness of the soil and building materials, the calculated median and logarithmic standard deviation of concrete compressive strain, rebar strain, and the out-of-plane shear stress in the base mat slab are shown for fault displacements of 5 cm to 30 cm in Table 3. For out-of-plane shear stress in the base mat slab, comparing medians evaluated from cases 1 to 4 and the result of median model case 0 shown in Table 4, the error is about 10%. Therefore, for statistical accuracy, the two-point estimation method is sufficient without using a detailed method, such as the Monte Carlo method. Since the overall trend of the analytical results in cases 1 to 4 was almost the same as that in case 0, an explanation will be omitted.

The logarithmic standard deviations of maximum concrete compressive strain and maximum rebar tensile strain in the base mat slab are almost 0.20 at fault displacement of 30 cm, but it could be larger after material yields. The logarithmic standard deviation of maximum out-of-plane shear stress in the base mat slab is about 0.10 for fault displacements of 0 cm to 30 cm, which is about one-half that of concrete compressive strain and rebar tensile strain.

The seismic PRA standard in Japan indicates that the logarithmic standard deviation is about 0.20 for maximum shear strain in shear walls and about 0.10 for maximum acceleration in each floor under earthquake motions. As for the quantitative value under the earthquake motions mentioned above, this variability study for fault displacement of 30 cm shows that the logarithmic standard deviations of strain are about 0.20 and those of the stress and deformation angle are about 0.10. But it is noted that while the response variability under earthquake motions is derived from a simple model as one element for one story, the response variability against fault displacement is based on a detailed model as two to three elements for one story.

Analyses are performed for cases 5 to 8 with the shear wave velocity of the surface soil and coefficient of friction between the soil and building as variables. In these analyses, the shear wave velocities of the surface soil for cases 5 and 6 are 250 m/s and 150 m/s, and coefficients of friction for cases 7 and 8 are 0.8 and 1.6. In addition, the coefficients of friction are set with reference to past experimental results [6].

Analytical results for cases 5 to 8 are shown in Table 2. Comparing cases 0, 5, and 6, although the uplift of the base mat slab increases due to weakening of constraining effect of the front and back soil, there is no significant difference for out-of-plane shear stress in the base mat slab. On the other hand, the out-of-plane shear stress of the building outer walls decreases as the stiffness of the surface soil decreases.

Comparing cases 0, 7 and 8, for the out-of-plane shear stress in the base mat slab, case 7, with the coefficient of friction 0.8, is the smallest. From the contact pressure contour plot of the base mat slab shown in Figure 5(b), it is thought that the uplift of the base mat slab is suppressed by the frictional

resistance between the side soil and building, but the reason why the out-of-plane shear stress in the base mat slab for case 8 with coefficient of friction 1.6 is larger than that for case 0 is unknown.

Based on the results in this section, the targeted failure mode is assumed the out-of-plane shear failure of the base mat slab. The variability of the out-of-plane shear stress in the base mat slab is shown in Table 4 and Table 5. Assuming a lognormal distribution, the logarithmic standard deviation is about 0.05 for shear wave velocity of the surface soil and about 0.15 for the coefficient of friction.

According to the results in this chapter, considering the variability of the structural response (βr = 0.10), the variability of shear wave velocity of the surface soil (βr = 0.05) and the variability of the coefficient of friction (βr = 0.15), the logarithmic standard deviation βr of the out-of-plane shear stress is assumed to be 0.20 from the square root of the sum of squares.

Table 3: Variability in Base Mat Slab (Cases 1 to 4)

Fault displacement	Concrete compressive strain		Rebar tensile strain		Out-of-plane shear stress	
	Median	Logarithmic standard deviation	Median	Logarithmic standard deviation	Median	Logarithmic standard deviation
cm	μ	μ	μ	μ	MPa	MPa
5	82.7	0.17	34.6	0.10	0.471	0.02
10	177	0.19	70.5	0.23	0.673	0.20
15	284	0.20	120	0.27	0.995	0.17
20	409	0.20	187	0.29	1.26	0.15
25	551	0.20	254	0.24	1.43	0.10
30	705	0.18	307	0.14	1.54	0.02

Table 4: Variability of Out-of-Plane Shear Stress in Base Mat Slab (Cases 5 to 6)

Case #	Out-of-plane shear stress in base mat slab (MPa)					
	10cm	20cm	30cm	40cm	50cm	60cm
0 (Vs of surface soil 500m/s)	0.6114	1.012	1.468	1.852	2.154	2.380
5 (Vs of surface soil 250m/s)	0.7295	1.094	1.528	1.917	2.187	2.365
6 (Vs of surface soil 150m/s)	0.8030	1.134	1.588	1.983	2.256	2.434
Logarithmic standard deviation	0.075	0.051	0.043	0.039	0.029	0.022

Table 5: Variability of Out-of-Plane Shear Stress in Base Mat Slab (Cases 7 to 8)

Case #	Out-of-plane shear stress in base mat slab (MPa)					
	10cm	20cm	30cm	40cm	50cm	60cm
0 (coefficient of friction 0.0)	0.6114	1.012	1.468	1.852	2.154	2.380
7 (coefficient of friction 0.8)	0.5654	0.9565	1.240	1.462	1.601	1.766
8 (coefficient of friction 1.6)	0.5629	1.238	1.668	1.942	2.277	2.641
Logarithmic standard deviation	0.081	0.115	0.121	0.116	0.143	0.160

5. STUDY OF EPISTEMIC UNCERTAINTIES

Uncertainty relating to fault displacement hazard defined as almost directly beneath building foundations is possibly classified as epistemic uncertainty because of the lack of relevant knowledge, including experimental and analytical data under the present circumstances. For example, uncertainties relating to fault types and fault geometries of location, dip angle, and slip direction presumably correspond to the epistemic one. Based on this current situation, some nonlinear soil-structure finite element analyses focusing on the above parameters are performed to obtain quantitative data relating to the epistemic uncertainty of building responses to fault displacement. Schematic images of analytical cases with epistemic uncertainty against dip-slip fault displacement are shown in Figure 6. In these analyses, the fault type of case 9 is a normal fault, fault location of case 10 is one quarter of the width of the base mat slab, and the dip angle of case 11 is 30 degrees. Uncertainty regarding fault location and dip angle are determined by reference to very few past experimental and analytical studies [7].

Analytical results for cases 9 to 11 are shown in Table 2. Comparing cases 0 and 9, although the maximum concrete compressive strain and the maximum rebar compressive strain in the base mat slab decrease, some rebars in the base mat slab yield under tension for case 9. This is because a normal fault occurs in a tensile stress field. Also, the out-of-plane shear stress of the building outer walls is very small because the front and back soil move away from the building. However, because of weakening of the constraining effect of the soil against the uplift of the base mat slab, the out-of-plane shear stress in the base mat slab increases.

Comparing cases 0 and 10, out-of-plane shear stress in the base mat slab for case 10 is slightly larger than that for case 0. This is because the uplift of the base mat slab is increased by shifting the fault position to the hanging wall.

Comparing cases 0 and 11, the out-of-plane shear stress in the base mat slab for case 11 is slightly smaller than that for case 0. From this result, it can be seen that the larger the angle formed with the fault plane, the greater the out-of-plane shear stress in the base mat slab. Also, out-of-plane shear stress in the building outer walls is small because the plasticity of soil around the building proceeds faster than for case 0, and the stress begins to decrease after the fault displacement exceeds 30 cm.

Based on the results of this chapter, the variability of out-of-plane shear stress in the base mat slab is

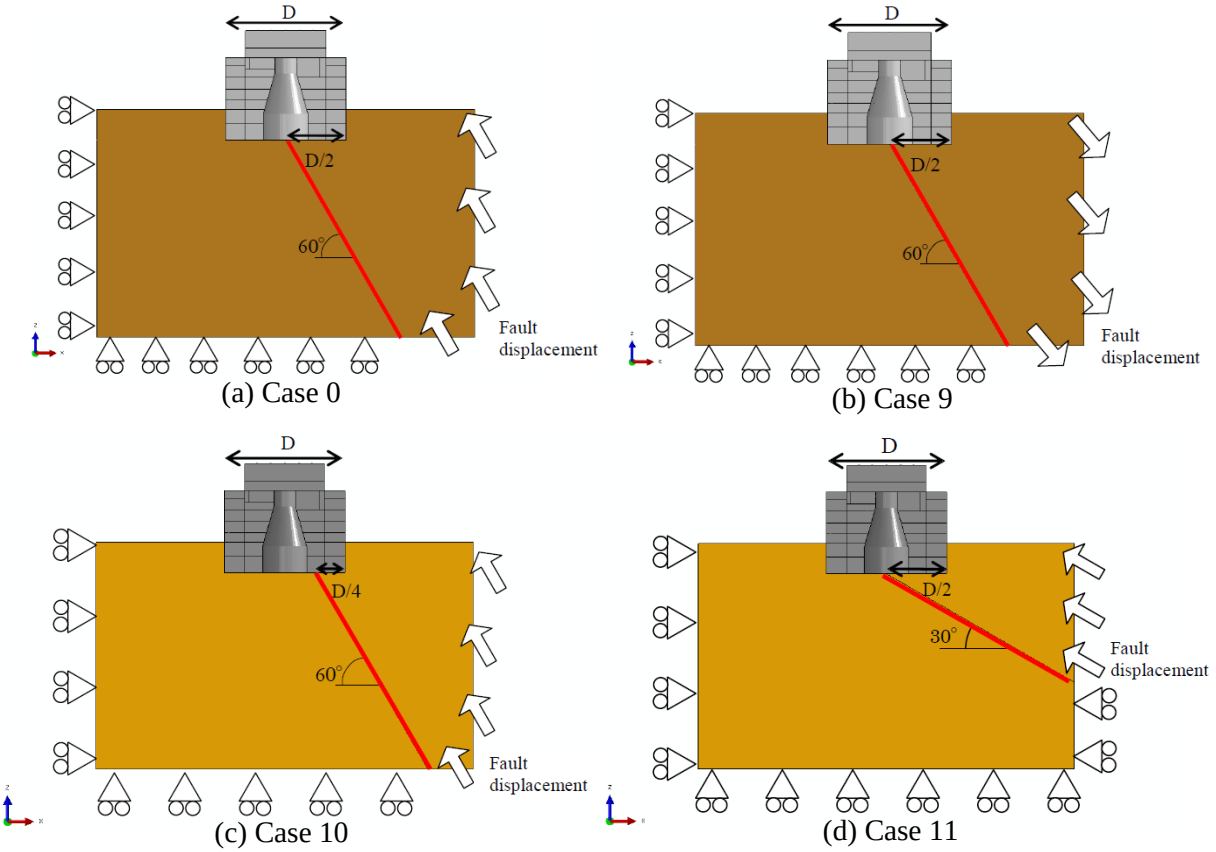

Figure 6: Schematic Image of Analytical Cases with Epistemic Uncertainty

Table 6: Variability of Out-of-Plane Shear Stress in the Base Mat Slab (Cases 9 to 11)

Case #	Out-of-plane shear stress in base mat slab (MPa)					
	10cm	20cm	30cm	40cm	50cm	60cm
0 (reverse fault, fault position D/2, dip angle 60°)	0.6114	1.012	1.468	1.852	2.154	2.380
9 (normal fault)	1.522	2.175	2.476	2.614	2.739	2.843
10 (fault position D/4)	0.9557	1.707	2.076	2.309	2.45	2.524
11 (dip angle 30°)	0.7469	0.9354	1.323	1.653	1.882	2.023
Logarithmic standard deviation	0.351	0.341	0.249	0.178	0.138	0.120

shown in Table 6. Assuming a lognormal distribution, logarithmic standard deviation βu of the base mat slab responses relating to epistemic uncertainty is assumed to be about 0.20 on average for fault displacements of 30 cm to 60 cm.

6. ANALYTICAL RESULTS FOR HARD ROCK SITES

For reference, it is assumed that the building is supported by hard rock ground whose shear wave velocity is 1500 m/s, and analyses are performed for cases 12 to 14 with the shear wave velocity of the surface soil and fault types as variables. In these analyses, the shear wave velocity of the surface soil for case 13 is 150 m/s and the fault type of case 14 is a normal fault.

Analytical results for cases 12 to 14 are shown in Table 2. Comparing case 12 to the others, the maximum compressive strain in the base mat slab and the out-of-plane shear stress of the building outer walls are particularly large. This is because the uplift of the base mat slab was suppressed by the surface hard soil, and the compression force in the direction orthogonal to the fault plane increased because of the reverse fault displacement. Because of this fact, since some shell elements at the edge of the base mat slab ware warped at fault displacement of 50 cm to 60 cm, there is a possibility that the calculation accuracy of the elements is insufficient.

Comparing cases 12 and 13, as uplift of the base mat slab increased from the weakening of the constraining effect of the front and back soil, the stress and strain reduced. This tendency is different from that of the soft rock site (comparison between cases 0 and 6). Since the actual soil around the building is usually soft backfill, the result of cases 13 and 6 is more realistic than that of cases 12 and 0. Consequently, the major failure mode against fault displacement can be judged as out-of-plane shear failure of the base mat slab.

Comparing cases 12 and 14, although the maximum concrete compressive strain and the maximum rebar compressive strain in the base mat slab decrease, some rebars in the base mat slab yield in tension for case 14. This tendency is similar to that of the soft rock site (comparison between cases 0

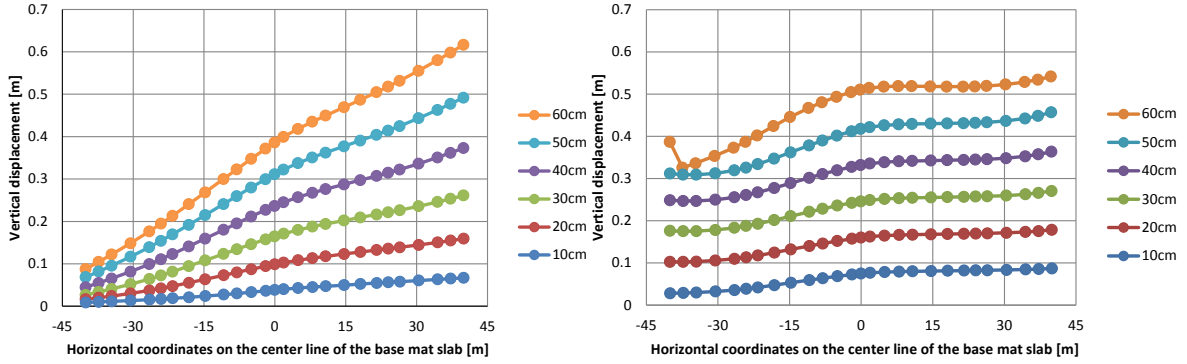

(a) Vertical Displacement

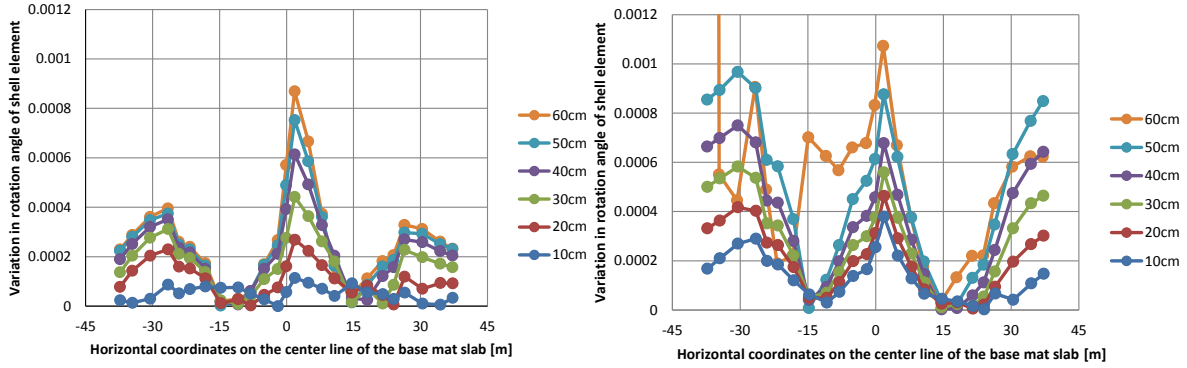

(b) Variation in Rotation Angle of Shell Element

Figure 7: Deformation Distribution of the Base Mat Slab (Left: Case 0, Right: Case 12)

and 9).

Focusing on the out-of-plane shear stress in the base mat slab, the result on the hard rock site (cases 12 to 14) is more severe than the soft rock site (cases 0, 6 and 9).

The deformation distribution of the base mat slab for the soft rock site (case 0) and the hard rock site (case 12) are shown in Figure 7. From the distribution of vertical displacement shown in Figure 7(a), the rigid body rotation of the building due to fault displacement can be seen. Additionally, this tendency is clearer in case 0 where the surface soil is less effective in suppressing the uplift of the base mat slab than in case 12.

Moreover, the rotation angle of each shell element for the base mat slab is calculated by the difference between the vertical displacement of adjacent nodes, and the distribution shown in Figure 7(b) is calculated from the difference between the adjacent rotation angle of each shell element for the base mat slab in order to eliminate the influence of the rigid body rotation. Figure 7(b) shows that the local out-of-plane deformation of the base mat slab gradually increases with fault displacement immediately above the fault plane. Furthermore, it is noteworthy that there is no significant difference in the out-of-plane deformation of the base mat slab between the soft rock site and the hard rock site. The local out-of-plane deformation at the edge of the base mat slab for case 12 is large because the hard rock site is more affected by the compression force in the direction orthogonal to the fault plane as described above.

7. FRAGILITY EVALUATION OF BASE MAT SLAB

The main failure mode against fault displacement for reactor buildings is shown in table 7. Based on the analytical results described above, the out-of-plane failure of the building outer walls will not become a dominant failure mode by considering realistic surface soil, that is, soft backfill. Hence, to prevent early dispersion of radioactive materials, the base mat slab is subject to a fragility evaluation from the viewpoint of prevention against large-scale damage for containment vessels.

Table 7: Main Failure Mode for Fault Displacement

Fault type	Effect on the building	Failure mode of outer wall	Failure mode of base mat slab
Normal	Dip-slip displacement	In-plane shear failure	Out-of-plane flexural/shear failure
Reverse	Dip-slip displacement	In-plane shear failure	Out-of-plane flexural/shear failure
	Compression force in the direction orthogonal to the fault plane	Out-of-plane flexural/shear failure (underground)	—※
Strike-slip	Strike-slip displacement	Out-of-plane flexural/shear failure (underground)	—※

※Although it generates stress, it will not reach the failure level.

Table 8: Conditional Failure Probability of Base Mat Slab

Fault displacement	Case 0		Case 12	
	inside shell	outside shell	inside shell	outside shell
cm	%	%	%	%
10	0.000	0.000	0.000	0.000
20	0.000	0.000	0.005	0.000
30	0.065	0.000	0.024	0.000
40	2.003	0.000	0.170	0.226
50	9.706	0.000	1.515	4.752
60	21.153	0.000	31.468	16.282

In order to quantify more precisely the prevention of large-scale damage to containment vessels with level 2 PRA in mind, this chapter presents the fragility evaluation with the following policy.

A: Inside the containment vessel (shell wall)

Focusing on the support function of the containment vessel and the RPV pedestal, the maximum out-of-plane shear stress of one element is used in the fragility evaluation.

B: Outside the containment vessel (shell wall)

Focusing on the stability of the reactor building as a whole, the average out-of-plane shear stress in the area (3 x 3 elements) corresponding to the thickness of the base mat slab, including one element with a maximum value, is used in the fragility evaluation. For reference, the results of the fragility evaluation using method A are also shown.

A preliminary fragility evaluation of the base mat slab for cases 0 and 12 is performed based on the analytical responses for fault displacement of 60 cm. Also, a logarithmic standard deviation of out-of-plane shear stress is assumed to be 0.20 based on the variability study of the aleatory uncertainties, and the median out-of-plane shear stress is directly derived from the analytical results up to a fault displacement of 60 cm.

The out-of-plane shear stress contour plot in the base mat slab inside and outside the containment vessel at a fault displacement of 50 cm is shown in Figure 8. The red frame outside the containment vessel in the contour plot shows the area of average stress. The conditional failure probability of the base mat slab is shown in Table 8. The conditional failure probability at a fault displacement of 60 cm is determined to be about 21% inside the containment vessel for soft rock sites and about 31% inside containment vessel for hard rock sites.

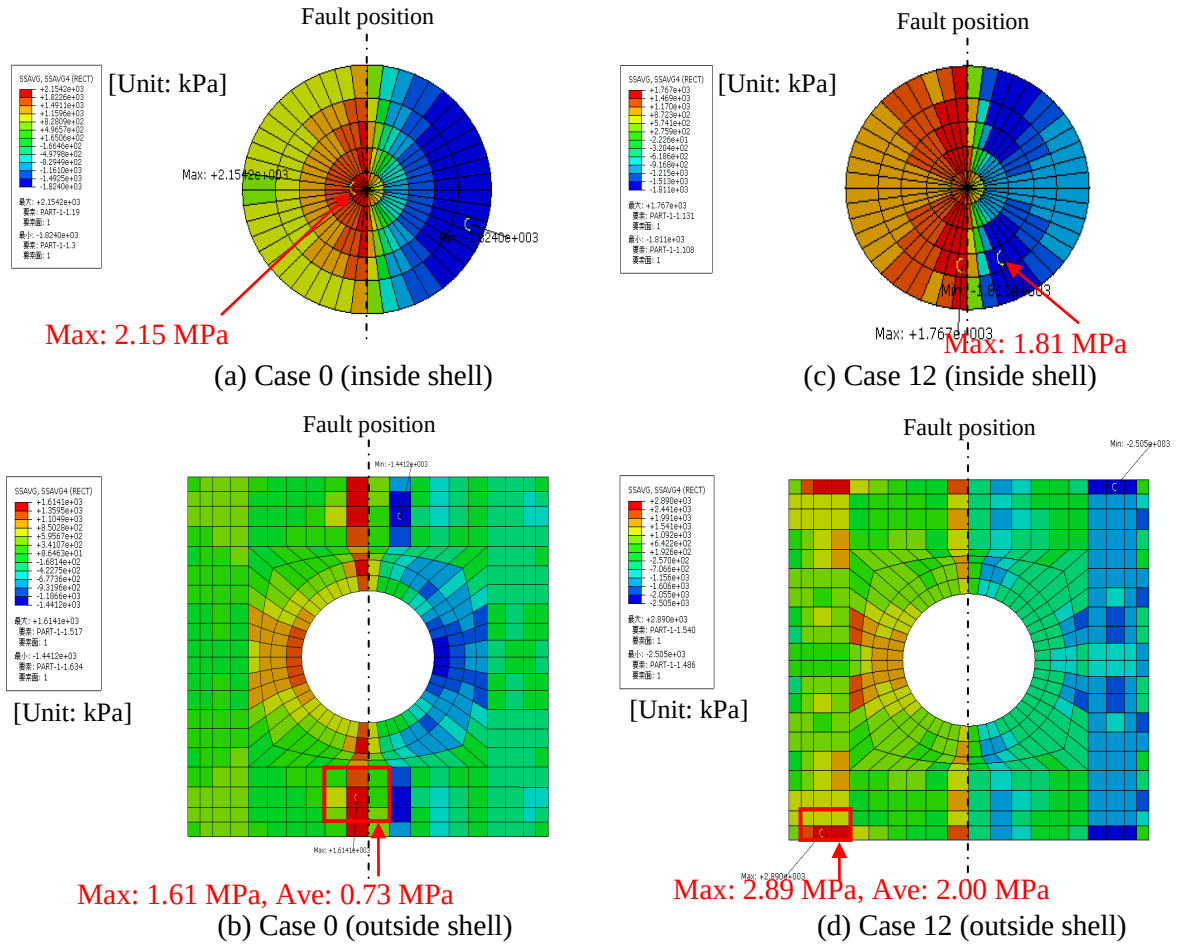

Figure 8: Out-of-plane Shear Stress Normal to Fault Inside and Outside Containment Vessel

Next, a median fragility curve with the aleatory uncertainty, such as logarithmic standard deviation βr, is obtained by the method of least squares to interpolate the conditional failure probabilities. Furthermore, a reliable fragility curve is evaluated with epistemic uncertainty, such as logarithmic standard deviation βu. Logarithmic standard deviation βu is determined to be 0.20 from the results in a previous chapter and 0.15 from a previous seismic PRA study [8].

The fragility curves with 50% reliability of the base mat slab against dip-slip fault displacement are shown in Figure 9. The hard rock site has a cliff edge whose failure probability rapidly increases at a fault displacement of 50 cm. The results of the fragility evaluation are shown in Table 9. The median fragility values for the base mat slab to fault displacement, that is, 50% failure probability, are 79 cm inside the containment vessel for soft rock sites and 63 cm inside the containment vessel for hard rock sites. The high confidence low probability of failure (HCLPF) values of the base mat slab to fault displacement is 32 cm inside the containment vessel for soft rock sites and 36 cm outside the containment vessel for hard rock sites.

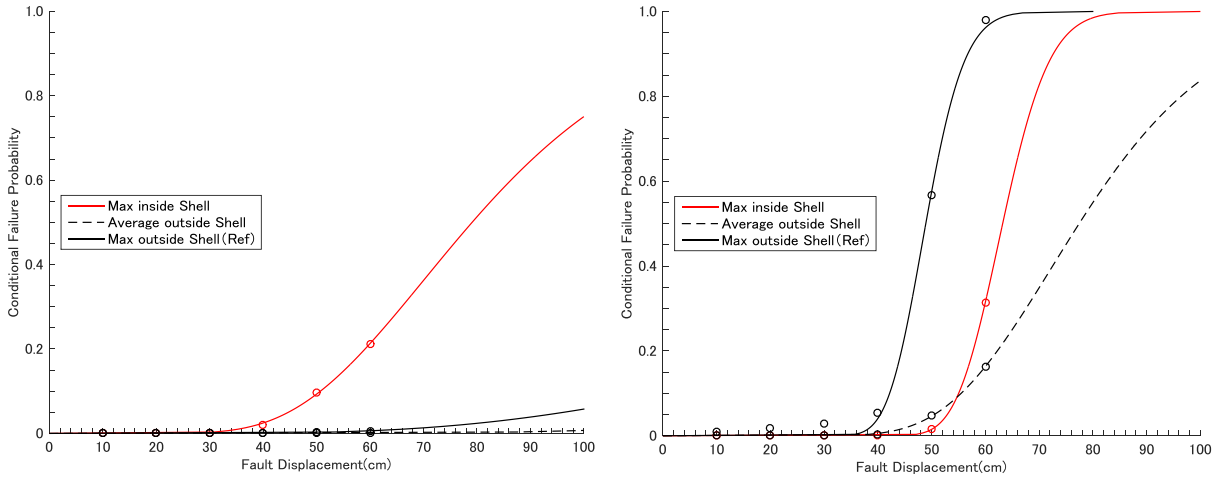

(a) Case 0 (b) Case 12

Figure 9: Fragility Curve with 50% Reliability

Table 9: Results of Fragility Evaluation

Position	Median		Logarithmic standard deviation		HCLPF	
	Case 0	Case 12	Case 0	Case 12	Case 0	Case 12
	cm	cm	-	-	cm	cm
Max inside shell	79	63	0.35	0.11	32	38
Average outside shell	357	77	0.52	0.26	110	36
Max outside shell (ref)	239	49	0.55	0.12	69	29

8. CONCLUSIONS AND FUTURE ISSUES

This paper has focused on obtaining basic fragility data for aleatory and epistemic uncertainties of structural responses for nuclear power plant buildings against fault displacement. A number of nonlinear soil-structure finite element analyses against relatively large fault displacements were performed taking into account the randomness of soil and building material properties, the uncertainty of contact parameters relating to friction between soil and the building, and the uncertainty of fault hazards such as fault types and geometries.

As a result, the logarithmic standard deviation of maximum out-of-plane shear stress in the base mat slab was assumed to be 0.20 based on the variability study of the aleatory uncertainties.

Furthermore, for plant-wide risk assessment from the defense-in-depth viewpoint, the preliminary fragility evaluation of the base mat slab up to a fault displacement of 60 cm that is twice the largest

recorded value of 30 cm and was performed not only considering the above variabilities as aleatory uncertainty but also the epistemic one relating to fault types and fault geometries of location, dip angle, and slip direction. From the results of the analytical parametric study of the epistemic uncertainties, the logarithmic standard deviation βu of base mat slab responses relating to epistemic uncertainty was assumed to be about 0.20 on average under these conditions against dip-slip fault displacement.

As a result, the median fragility values of the base mat slab to fault displacement, that is, 50% failure probability, are 79 cm inside the containment vessel for soft rock sites and 63 cm inside the containment vessel for hard rock sites. The high confidence low probability of failure (HCLPF) values of the base mat slab to fault displacement is 32 cm inside the containment vessel for soft rock sites and 36 cm outside the containment vessel for hard rock sites.

However, these preliminary fragility results were obtained from very limited analytical conditions of a dip-slip fault, specific soil material properties, and an assumed boundary conditions between the soil and building. Therefore, to obtain more generic and standard data for a fragility evaluation against fault displacement, the following issues should be investigated and discussed in the future.

- Uncertainty of fault type such as strike-slip fault

References

[1] On-site Fault Assessment Method Review Committee in Japan Nuclear Safety Institute (2013). *Assessment Methods for Nuclear Power Plant against Fault Displacement*, JANSI-FDE-03 rev.1, http://www.genanshin.jp/archive/sitefault.

[2] Tsuji, H., Kanechika, M., Mihara, Y. and Ishiki, K. (2016). "Fragility Evaluation with Aleatory and Epistemic Uncertainty against Fault Displacement for Nuclear Power Plant Buildings," PSAM 13, Seoul, Korea.

[3] Lee, J. and Fenves, G. L. (1998). "A Plastic-Damage Concrete Model for Earthquake Analysis of Dams," *Earthquake Engineering and Structural Dynamics*, vol.27, pp. 937-956.

[4] Kumagai, H., Nukui, Y., Imamura, A., Terayama, T., Hagiwara, T. and Kojima, I. (2011). "Out-of-plane Ultimate Shear Strength of RC Mat-slab Foundations," *Journal of structural and construction Engineering, Architectural Institute of Japan*, vol.76, no.659, pp. 131-140 (in Japanese).

[5] Atomic Energy Society of Japan (2007). *A Standard for Procedure of Seismic Probabilistic Safety Assessment for Nuclear Power Plants: 2007, A Standard of the Atomic Energy Society of Japan*, AESJ-SC-P006:2007 (in Japanese).

[6] Shimada, T., Suzuki, Y., Takei, K., Yano, T., Sato, H., Furuno, Y. and Eguchi, M. (2015). "Experimental assessment of shear transmitting mechanism between underground outer wall of embedded nuclear power plants and lateral soil: Part 1 and Part 2," *Summaries of technical papers of annual meeting Architectural Institute of Japan*, pp. 1091-1094 (in Japanese).

[7] Solhmirzaei, R., Soroush, A. and Mortazav Zanjani, M. (2012). "Fault Rupture Propagation through Level Ground and Sloping Sand Layers," 4148, 15WCEE, Lisbon, Portugal.

[8] Mihara, Y., Fushimi, M., Miyazaki, S. and Sugita, H. (2007). "Study on Epistemic Uncertainties in Fragility Evaluation of NPP Buildings: Part 3," *Summaries of technical papers of annual meeting Architectural Institute of Japan*, pp. 1083-1084 (in Japanese).